LANDSLIDING AT CEMENT CREEK, KLUANE RANGES, SOUTHWESTERN YUKON

M. A. Power
Department of Physics
University of Alberta
Edmonton, Alberta

POWER, M.A., 1988. Landsliding at Cement Creek, Kluane Ranges, southwestern Yukon; in Yukon Geology, Vol. 2; Exploration and Geological Services Division, Yukon, Indian and Northern Affairs Canada, p. 51 - 60.

ABSTRACT

A large block slide affecting an area of approximately 1.0 square km was reported to have occurred on Cement Creek Y.T. (115 G 5) between February 15 and March 15, 1983. Landsliding is confined to basaltic andesites in the lower unit of the Wrangell Lavas. Hydrothermal alteration of flow-top breccias and the tilting of strata towards an open face bordering Cement Creek predispose rock to slip along bedding planes. Surveys conducted during June to August 1986 detected displacements of 10-12 cm during an 8 week period. Seismic refraction and electrical resistivity surveys conducted on the slide mass suggest that most ground failure was caused by strong ground motion during an initial episode of rapid displacement and that the rupture surface lies beneath the lower limit of permafrost. Groundwater accumulation on and above the rupture surface followed by landslide initiation during a burst of low magnitude seismicity is suggested as a slide mechanism.

RÉSUMÉ

Un vaste éboulement touchant une superficie d'environ 1,0 km² a été signalé à Cement Creek, dans le territoire du Yukon (115 G 5); il aurait eu lieu entre le 15 février et le 15 mars 1983. Ce glissement de terrain est confiné aux andésites basaltiques de l'unité inférieure des laves de Wrangell. L'altération hydrothermale des brèches supérieures d'épanchement et l'inclinaison des strates en direction d'une face exposée bordant le ruisseau Cement favorisent les glissements de la roche selon les plans de stratification. Des levés réalisés de juin à août 1986 ont permis de déceler des déplacements de 10 à 12 cm sur une période de 8 semaines. Les levés de sismique-réfraction et de résistivité électrique dont a fait l'objet la masse en mouvement suggèrent qu'en majeure partie, les glissements de terrain ont été causés par de forts mouvements du sol durant un épisode initial de déplacement rapide, et que la surface de rupture se trouve au-dessous de la limite inférieure du pergélisol. On propose, comme mécanisme de glissement, l'accumulation des eaux souterraines à la surface et au-dessus de la surface de rupture, puis le déclenchement du glissement de terrain durant un épisode de sismicité de faible magnitude.

INTRODUCTION

During the winter of 1983 a large landslide was reported at Cement Creek in the St. Elias Mountains, southwestern Yukon (115 G 5, Fig. 1). D. Makkonen, a pilot with Trans North Air Ltd. in Haines Junction reported that the landslide occurred between February 15 and March 15, 1983 and affected an area approximately 1 km in diameter. Some later observers felt that uplift might be occurring since the feature was centred on a domal hill and accompanied by radial ground cracks.

Investigations were conducted during June-August, 1986 to determine the rate and sense of deformation and its cause. A microgeodetic survey grid and a series of trilateration stations were constructed to measure the rate of displacement of individual parts of the landslide. Geological mapping, and logging and sampling of exposed sections were conducted to delineate the factors controlling the landslide. Seismic refraction and electrical resistivity surveys were conducted to delineate the geological controls on the landslide and to gain information on the geotechnical properties of the material in the slide mass. A topographic survey was undertaken to permit subsequent slope stability analysis.

GEOLOGY

Cement Creek is located in the northwest St. Elias Mountains. The area is underlain by Permo-Pennsylvanian through Pliocene volcanic and sedimentary rocks assigned to the Wrangellia Suspect Terrane (Campbell and Dodds, 1979). The area has been mapped by Muller (1967), Dodds (1979), and Skulski and Francis (1986). The general geology of the area near the Cement Creek landslide is shown in Figure 2. Pleistocene and Holocene surficial deposits cover four stratigraphic rock units.

The Permo-Pennsylvanian Station Creek Formation is exposed at the northern edge of the map area, in the core of a plunging anticline as a series of rusty-weathering, slightly vesicular basalt flows 3-6 m thick.

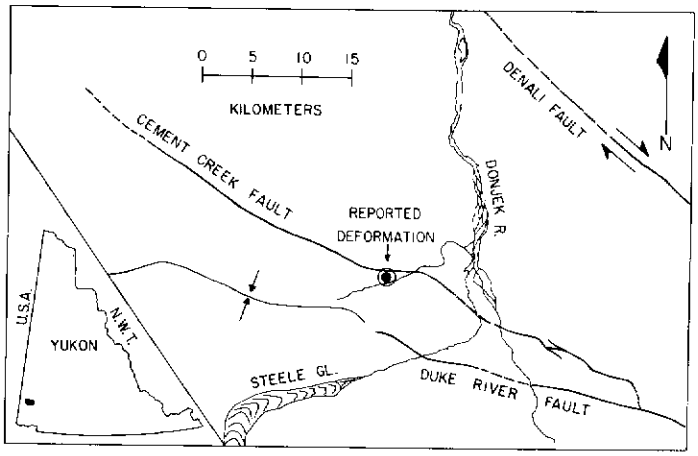

Figure 1. Location of ground failure reported in 1983.

The overlying Paleocene to Miocene Amphitheatre Formation is an assemblage of continental clastic rocks (Eisbacher, 1975). The succession exposed at Cement Creek includes polymictic conglomerate with intermittent cross-stratified sandstone and coal-rich siltstone. These rocks are well indurated and resistant to weathering except where altered near the Cement Creek fault.

The Miocene to Pliocene Wrangell Lavas cover most of the map area and from an engineering standpoint are the most hazardous rocks in this portion of the St. Elias Mountains. The petrology and tectonic setting of these rocks has been described by Muller (1967), Souther and Stanciu (1975), and Skulski and Francis (1986). The

Cement Creek landslide is underlain by the lower Wrangell Lavas (Dodds, 1979). A 150 m section immediately east of the main slide consists of basaltic andesite flows, 5-15 m thick, with rusty weathering flow-top breccias. Two 3-5 m thick syntectonic felsite dykes cut bedding at a slight angle at the base and middle of the section.

The breccias capping the flows consist of altered purple to red brown clasts 5-30 cm long in an altered matrix of montmorillonite, kaolinite, muscovite and local chlorite. Rare voids in these horizons are filled by quartz and actinolite. The intense hydrothermal alteration in the flow top breccias presumably reflects their great initial permeability. They form ideal landslide rupture surfaces since the flow tops are smooth and the alteration products in the breccias render them mechanically weaker.

Hydrothermal alteration has also proceded along joint sets perpendicular to a fold axis affecting rocks in the slide mass and may have weakened them at depth. The major medial fissure bisecting the slide mass in Figures 3(c), 3(d) and Figure 4, has walls which are intensely altered and is faintly visible as an a-c joint in Figure 3(b). Other major cracks near the toe of the slide are controlled by jointing. Hydrothermal alteration is also localized along the Cement Creek fault and in a discordant nearly vertical band of kaolinite which parallels the northwest-trending creek in the west of the map area.

The Wrangell Lavas have been intruded by syntectonic dacites, rhyolites and trachytes (Souther and Stanciu, 1975; Skulski and Francis, 1986). A plug of light grey rhyolite or dacite, dated by Muller (1967) as Pliocene to Recent, outcrops north of the Cement Creek fault (Fig. 2). No Amphitheatre strata were found between this unit and the Cement Creek Fault, thus it may be fault bounded to the south. The intrusion could be as old as Miocene (Dodds, 1979) although Muller speculates that these rocks are petrogenetically and perhaps temporally related to younger rocks such as the White River Ash (1400 years B.P.).

Glacial till and periglacial deposits of clay and silt overlie bedrock throughout the map area. Thicknesses on up-valley facing slopes are 0.5-2 m thick, but reach 5 m in the headwall scarp on the lee side of the slide mass.

STRUCTURE

Structure in the map area of Figure 2 is dominated by two elements: the Cement Creek fault and a pericline immediately south of it.

The Cement Creek fault is an extension of the Wade Mountain fault zone of Read and Monger (1975), originally mapped by Souther and Stanciu (1975). Skulski and Francis (1986) refer to it as the "Cement Creek Fault" and this nomenclature is retained. Including the Wade Mountain extension, this fault runs from the Burwash Uplands to the outwash plain of the Klutlan Glacier where it disappears beneath Holocene deposits. It is vertical, and shows no topographic expression. This, and the fact it splays from the Duke River Fault suggest that right lateral strike slip displacement has occurred along it. Where it outcrops in the eastern part of Figure 3, it is a steeply-dipping, 20 m wide zone of sheared and bleached rock. In places bedding has been folded about nearly horizontal axes, suggesting some local dip slip displacement. No obvious indications of recent movement were observed at Cement Creek. Souther and Stanciu (1975) documented the tilting of both bedrock and overlying Plio-Pleistocene surficial deposits near the fault at Bull Creek and therefore it may still be active.

An east-striking synclinal pericline is located south of the Cement Creek fault (Fig. 2). At its east and west ends, the fold axis plunges at 15° towards a depression located north of Cement Creek. The influence of this structure on landslide kinematics is discussed in the context of the slide morphology (see below).

The Cement Creek landslide occurred in a region of high historical seismicity coincident with the Duke River, Shakwak and Totschunda faults (Horner, 1983). Earthquakes up to M = 6.0 have occurred near the Duke River Fault and microseismicity is high. The regional seismograph network is capable of detecting events down to M = 2.0, and locating them to within 20 km (Horner, 1983; Clague, 1979). Seismicity during the period in which the landslide is bracketed is summarized in Table 1. An earthquake of M = 5.0 was recorded within 20 km of the slide on March 30, 1983. The region of after-

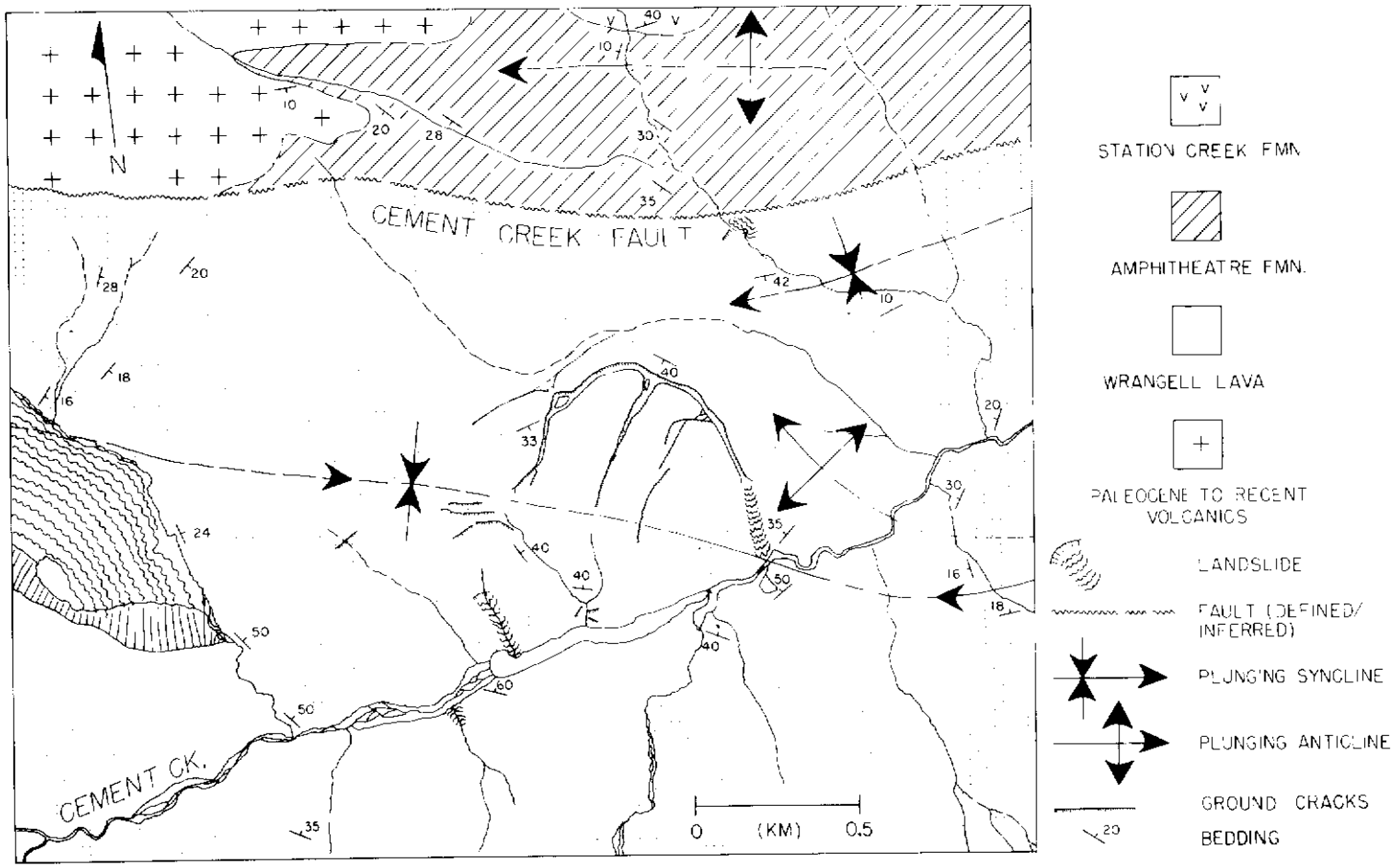

Figure 2. Geology and geomorphology of the Cement Creek area.

TABLE I

Recorded Seismic Events within 160 Km of Cement Creek Slide Between 14 February 1983 and 15 March 1983.

DATE/TIME (U.T)	MAGNITUDE (M_S)	DISTANCE (KM)
7 MAR 83/16:18:25	2.7	90
8 MAR 83/12:12:42	3.8	150
9 MAR 83/12:28:58	3.1	75
1 MAR 83/22:43:26	2.7	110
13 MAR 83/02:45:49	2.3	110

(Sources: Earth Physics Branch/NEIS)

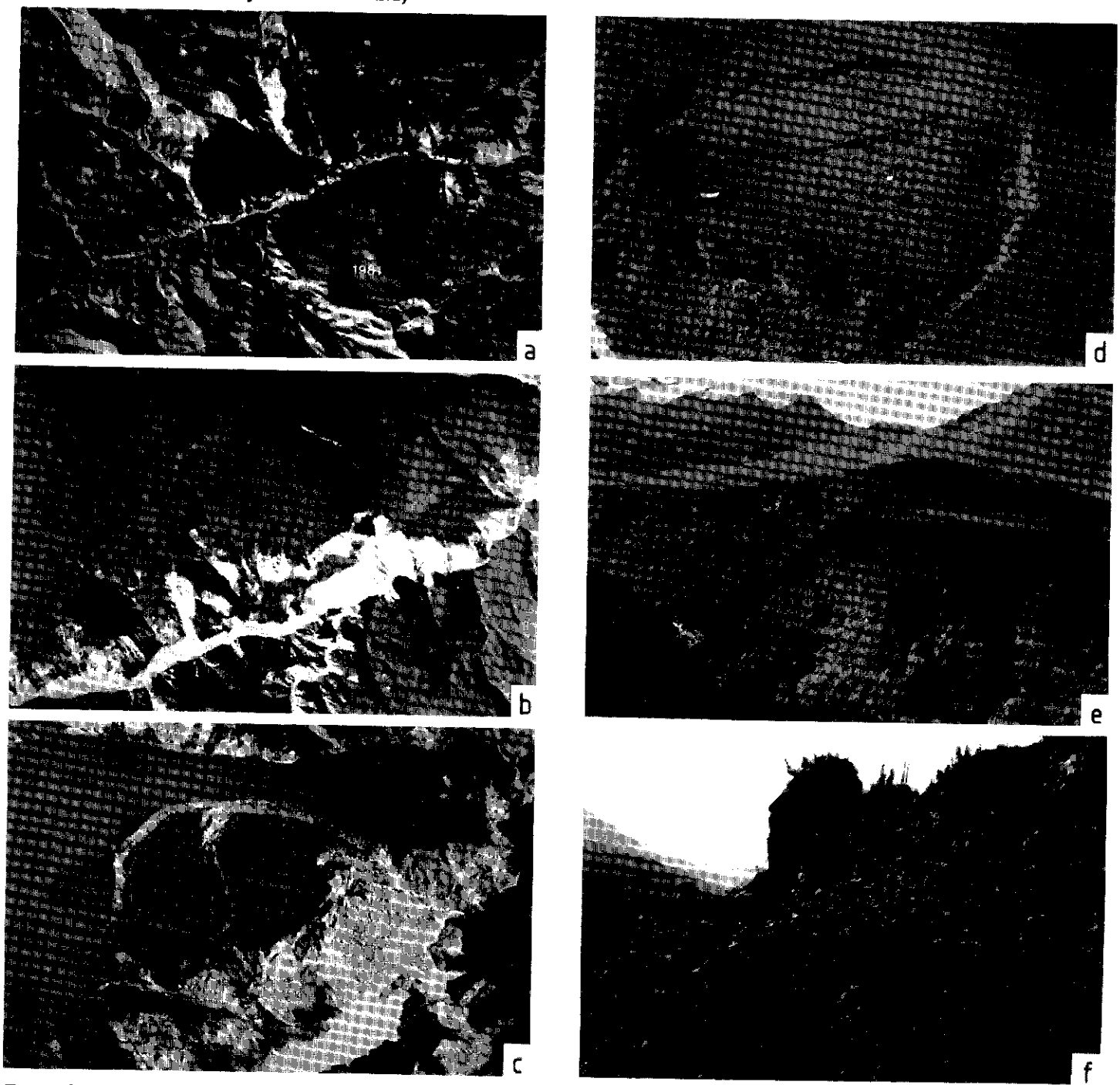

Figure 3. (a) Airphotograph of Cement Creek area (1981). Cement Creek runs west-southwest to east-southeast across the photgraph; and the plateau on which landsliding occurred is in the centre, bordering Cement Creek to the north. (b) Enlargment of the same airphotograph showing the incipient landslide. (c) - (d) Main slide and accessory damage viewed from the southwest and east respectively. (e) View of the main slide from the south. Wrangell strata, visible in foreground, dip towards Cement Creek in the slide area. (f) View of the toe of the slide. Slip surface outcrops as a ledge overlain by debris and intact spires of rock.

shocks included the Cement Creek site and low magnitude foreshocks (i.e., M 2.0) possibly triggered the landslide.

GEOMORPHOLOGY

Landsliding and related ground failure at Cement Creek is confined to the south margin of the triangular plateau in the centre of Figure 3(a). The landslide is 850 m wide, centred on a domal hill protruding 110 m above the plateau. Holocene down-cutting by Cement Creek has incised a 90 m deep canyon which forms the south boundary of the plateau. Landsliding occurs where bedding dips out of this open face. The landslide is a block slide with breakup of the slide mass occurring only at the toe. There, large spires of rock up to 60 m high have separated from the slide mass. The slide mass is perched on a bedrock ledge outcropping half way up the exposed face. It is evidently intact since large blocks of slide debris are supported by it (Fig. 3(f)). Maximum landslide displacements appear to be 30 or 40 m.

This landslide is unusual in that displacements have a rotational component and the headwall scarp has developed midway up the hill comprising the slide mass. Both of these effects can be ascribed to bedding control.

The morphology of the headwall scarp and the distribution of ground cracks indicate that both slight clockwise rotation and downslope translation occurred. The headwall scarp varies in width along strike, narrowing from 70 m wide in the east to 20 cm wide on the west flank where it eventually disappears. This effect is produced by clockwise rotation of the slide mass away from the scarp. The distribution of major cracks on and adjacent to the landslide is shown in Figure 4. The trend of these cracks varies progressively from east to west with cracks nearest the toe being parallel to the exposed face and those higher up, oblique to it. This suggests that as blocks move down the rupture surface, they are progressively rotated in a clockwise sense.

For reasons discussed previously, bedding is thought to be a significant factor controlling landsliding of these rocks. The displacement suggested by the crack pattern is consistent with oblique slip down bedding in the north limb of the synclinal pericline dominating the local structure. Dip slip would be inhibited by the inflection of bedding at the fold axis, and the flexure of bedding at the depression of the pericline could account for the rotational component of motion as shown in Figure 5. This would occur as the gradient in the direction of the fold axis was progressively reduced in approaching the depression of the pericline. The component of motion directed

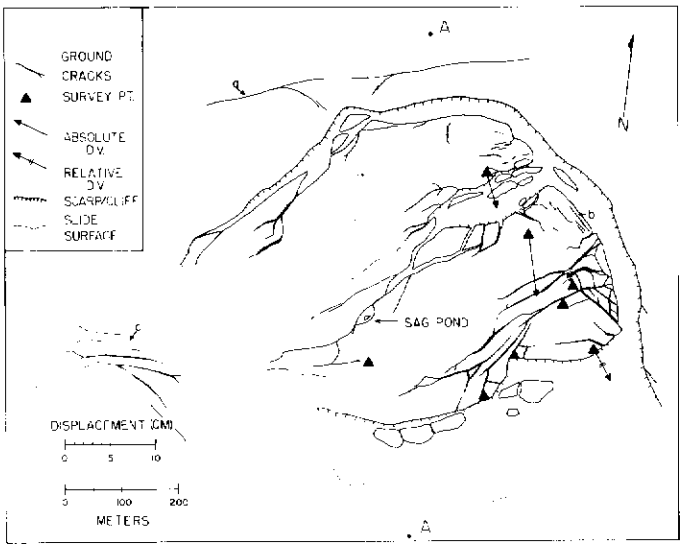

Figure 4. Map of principal ground cracks and displacement vectors. Three types of cracks are indicated: (a) Ground cracks formed prior to 1983; (b) Cracks developed on north face of the slide mass as a consequence of block rotation; (c) Cracks unaccompanied by landsliding.

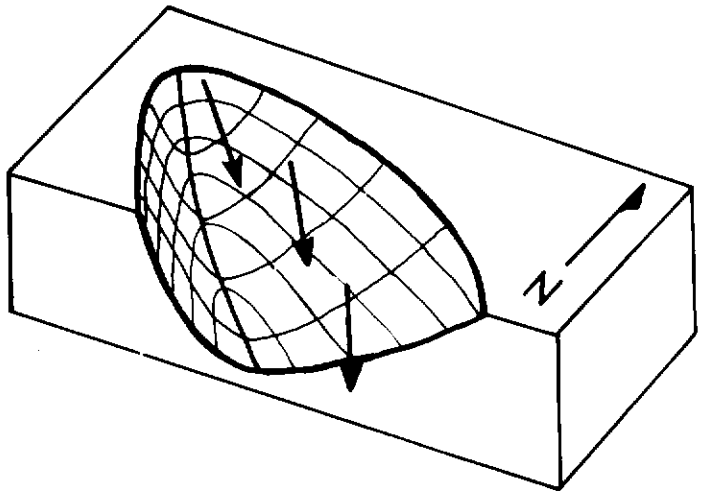

Figure 5. Schematic diagram of slide surface. Displacement vectors are rotated because of changes in gradient, primarily along the fold axis.

along the axis would decrease while that perpendicular to it would be relatively unaffected. A net rotation results.

The peak velocity of the landslide could not have been great; no evidence of splash is visible on the slopes of the south wall of the canyon. The debris fan dammed Cement Creek, impounding a lake 1 km long behind it, but the dam is permeable; during a dry spell in June, 1986, the creek's discharge percolated through the barrier with no surface flow. Levees approximately 10 m high border the creek where it cuts through the toe of the slide and the stream is clearly not competent to remove this debris.

The slip surface of the landslide is a prominent ledge, visible in Figure 3(b) as a tree covered ramp on the front face of the slide and as it appeared in 1986 in Figure 3(f). Debris in the toe of the slide has obliterated all evidence of any prior tree cover, but the ledge is still intact and able to support large spires of rock which have ridden out on it. It consists of relatively unaltered lower Wrangell lava flows and is oriented consistently with nearby bedding. That portion of the slip surface visible in the headwall scarp dips at approximately 50° towards the toe of the slide. Rock exposed here is highly altered with bedding largely obliterated. The dip of the slip surface is greater than that of bedding, indicating that the rupture surface departs from bedding at depth, cutting up to the headwall scarp.

The upper part of the rupture surface appears to be concave as some evidence exists that the north slope of the slide mass has been rotated to vertical. This is afforded by a series of ground cracks cutting across the steep north face of the hill involved in the landslide (b in Fig. 4). These cracks are at most 40 cm deep and involve only sod and the upper layer of the soil horizon. They have not developed on the stationary portion of the hill below the headwall scarp and appear to result from solifluction of the top layer of permafrost during seasonal thawing. The fact that these features are present only on the back face of the slide mass and not on the hill below the headwall scarp suggests that the north face of the slide has rotated through an angle sufficient to to destabilize the overlying vegetation. A composite cross section incorporating the results of both topographic and geophysical surveys is displayed in Figure 6.

In addition to the solifluction cracks, three other broad classes of cracks are visible on, and near the landslide. These include cracks predating the 1983 landslide, surficial and deep cracks formed during the 1983 slide, and others dating from 1983 west of the landslide.

A series of cracks, clearly older than those developed during 1983, are found north of the landslide at the break in slope between the hill and plateau (a in Fig. 4). These, individually up to 100 m long, form a linear en echelon array 570 m long. They strike across the northwest side of the landslide, deviating only near a kink in the headwall scarp. They do not wrap around the back of the slide as would be expected if they reflected headward migration of the slip surface; instead they continue northeast and disappear in a stream bed at

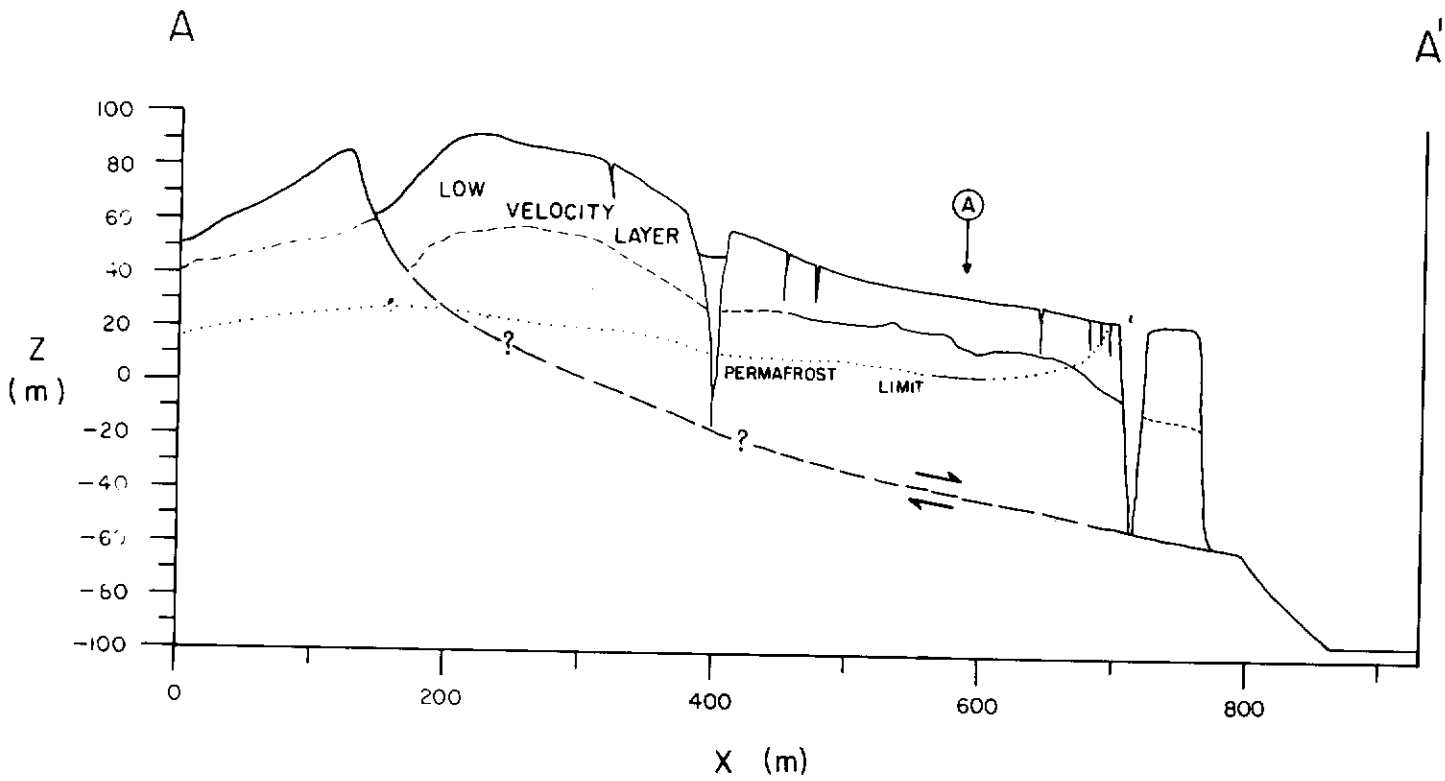

Figure 6. Composite cross section integrating the results of geophysical and topographic surveys. Low velocity layer of weathered rock and surficial deposits mapped from seismic surveys. Permafrost limit mapped from electrical resistivity soundings. Location of slip surface determined from topographic surveys. Line of section indicated in Figure 4. Inferred boundaries are dashed.

the foot of the hill on which the slide is located. The cracks expose bare earth and are up to 40 cm deep with weathered and partially overgrown sides. The linearity of these cracks, irrespective of local topography, coupled with their length and depth argue against their being some unusual frost effect. They are faintly visible on enlargements of airphotographs shot in 1943, 1972 and 1981. They appear to parallel some anisotropy in bedrock and may have developed during a landslide prior to 1943.

The second class of ground cracks are those formed by the 1983 landslide. These can be subdivided into two categories on the basis of apparent depth. Most are rooted at depths no greater than 10 - 20 m and are most abundant near the toe of the landslide. Geophysical evidence, discussed below, suggests that they do not extend to the slip surface. The second class includes larger, longer cracks at least 40 m deep extending down to the slip surface. These cracks separate major blocks in the landslide which to some degree move independently of each other. This effect was detected in measurements of absolute displacement of points on either side of the medial crack which bisects the slide (Fig. 3(b), 3(c), 4).

The third class of cracks is a series which formed in 1983 immediately west of the landslide. These are 5-8 m deep and are clustered on the edge of a small spur immediately west of the main slide (bottom right quadrant of Figure 3(b)). They do not appear to be structurally connected to those on the main slide; the headwall scarp crack ends about 100 m north of this site and these cracks strike perpendicular to it. No evidence of deep seated bedrock displacement was observed.

The area involved in the 1983 landslide appears to have undergone mass movement prior to 1943. The incipient trace of the headwall scarp and medial crack is faintly visible in airphotography shot prior in 1943, 1972 and 1981. The ledge which forms the slip surface and underlies the toe of the slide is tree covered in enlargements of 1981 airphotographs, suggesting that the landslide has been inactive for at least a century (Fig. 3(b)). Displacement prior to 1983 appears to have been minimal since the slide mass remained essentially intact and the incipient headwall scarp was approximately 10 m wide.

DEFORMATION RATES

In order to ascertain whether motion of all or part of the landslide was still occurring, a series of survey stations were installed to measure absolute and relative deformation rates. Motion relative to the presumably stationary plateau was monitored by means of a microgeodetic survey network (Fig.7). Relative displacement across apparently active cracks was measured using the method of trilateral signs outlined by Ter Stepanian (1980). Lastly, an attempt was made to measure the rate of crack propagation by means of pegs offset perpendicularly from the tips of individual cracks. Significant displacement was detected only in the first two of these studies.

The microgeodetic survey grid consisted of three stations sited around the perimeter of the landslide. At each station, motion of one or two sites on the slide was measured with respect to two fixed points on the plateau. Survey sites consisted of a tripod positioned over a hub and anchored into the permafrost. During each survey, the distance along three sides of the triangle formed by the two points off the slide and the one on it were measured using a Sokkisha Red-1A electronic distance measuring device (EDM). The vertical angles between points 1, 2 and 3, their respective reference points and the sites on the slide were measured using a Kern DKM-II triangulation theodolite. EDM measurements were corrected for air temperature and pressure; no corrections for refraction were made to angular measurements. The position of each station on the slide was then calculated relative to a rectangular coordinate system centred at each of points 1, 2 and 3, with the positive X-axes being the horizontal projections of the vectors 1-1A, 2-2A and 3-3A and the Y-axes pointing towards the landslide in the horizontal plane. The apparent motion of points on the landslide was projected into the horizontal plane and plotted in Figure 8.

The sources and magnitude of error in these surveys strongly influenced the significance of the results. EDM standard error was less than 1 cm over the distances used in the network. Systematic distance measurement error was overcome by normalizing the measurements against the repeated measurements of the distance between the fixed reference points. Refraction error was negligible

since angles never exceeded 10°. Levelling error was significant; tripods were prone to shifting between shots and 30"s of arc was assigned as the angular measurement error. EDM and angular measurement error translated into a maximum combined error of +/- 3.0 cm in the position of any point in the plane of projection.

The criteria used to establish true displacement were: (1) initial and final points be separated by at least 6.0 cm; and (2) the overall trend of the apparent motion be smooth. The apparent random motion of points 1B and 3B are therefore attributed to frost heave or some other site specific effect not related to landsliding. Motion was detected at sites 2B and 2C where displacement vectors were 10 ± 6 and 12 ± 6 cm, respectively.

Relative displacement across major and/or apparently active cracks was measured using the method of trilateral signs outlined by Ter Stepanian (1980). Measurement error was calculated using extreme values rather than the geometrical construction he developed. Relative displacements were detected across cracks at sites T-1 and T-4 (Fig. 7) and are plotted in Figure 8.

Absolute displacement at sites 2B and 2C is consistent with the overall pattern of ground cracks in the slide mass (Fig 7.) and with observations on the activity of the landslide made by the field party. The clockwise sense of rotation of the displacement vectors matches that suggested by the ground cracks. No indications of significant motion were apparent in 1986. If the slide was active, unstable debris in the toe of the slide should have been displaced. Particular attention was paid to a large block perched near the front edge of the ledge forming the slide surface (Fig. 3(f)) which leaned towards the creek at about 15°. No motion of this, or any other debris was noted. The small amount of detected displacement was in rocks resting on the steepest portions of the rupture surface. This may be a seasonal feature caused by the infiltration of groundwater from summer run-off. Relative displacement at T-1 is due to the separation of an island of trees and frozen surficial deposits from the slide mass in the toe. Its displacement vector reflects the local orientation of the slip surface in the immediate area and not its overall morphology. Deep seated creep appears to still be occurring in the slide mass, but this process cannot account for the observed ground failure.

GEOPHYSICAL SURVEYS

Refraction seismic and electrical resistivity surveys were conducted to map the rupture surface at depth and to obtain data on the geotechnical properties of the slide material. The philosophy behind such investigations is outlined by Muller (1977). Fracturing of rock in a slide mass lowers P-wave velocity and allows ground water to percolate to the slip surface. Often an impermeable gouge layer

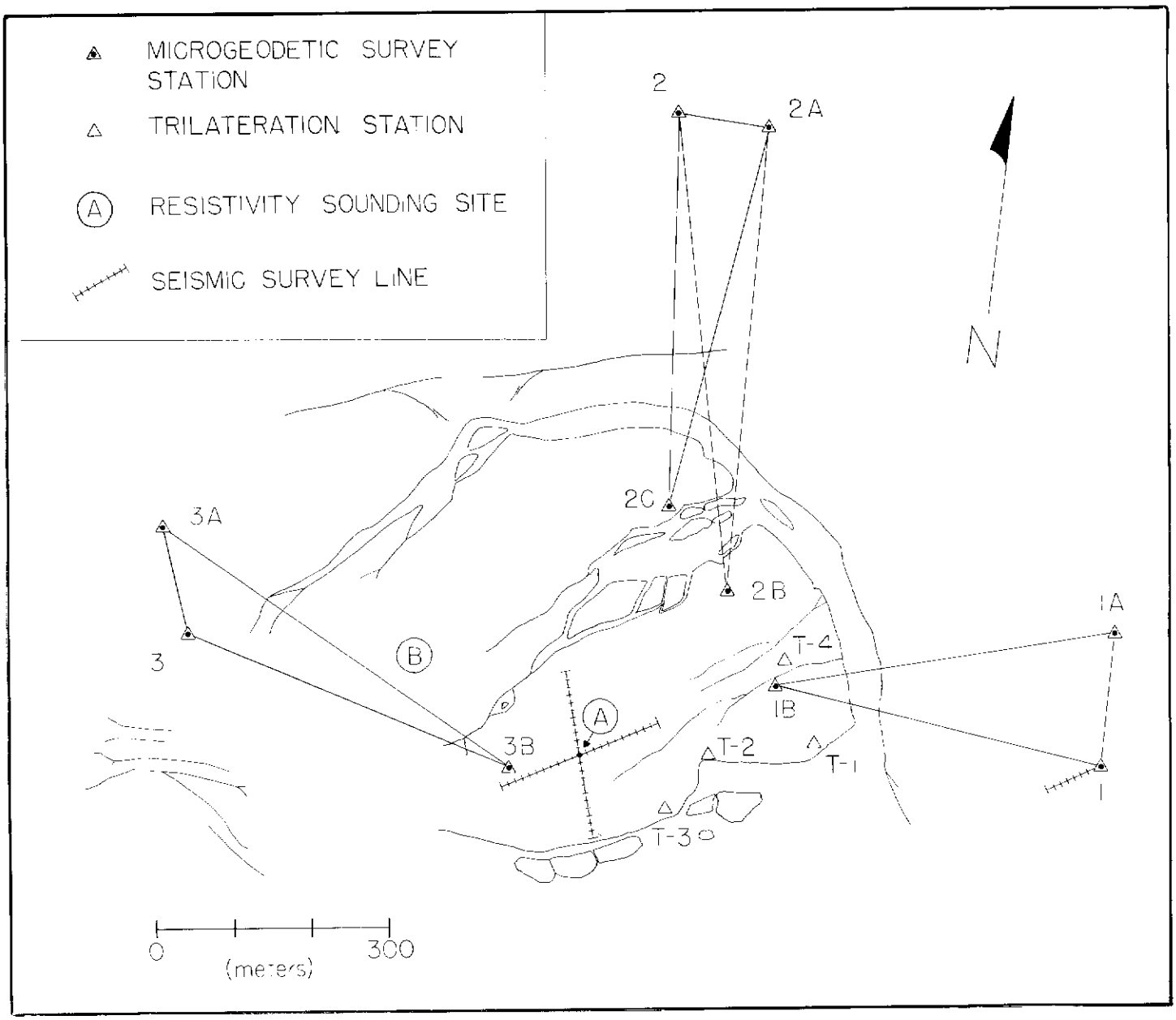

Figure 7. Location of microgeodetic survey grid and geophysical survey sites.

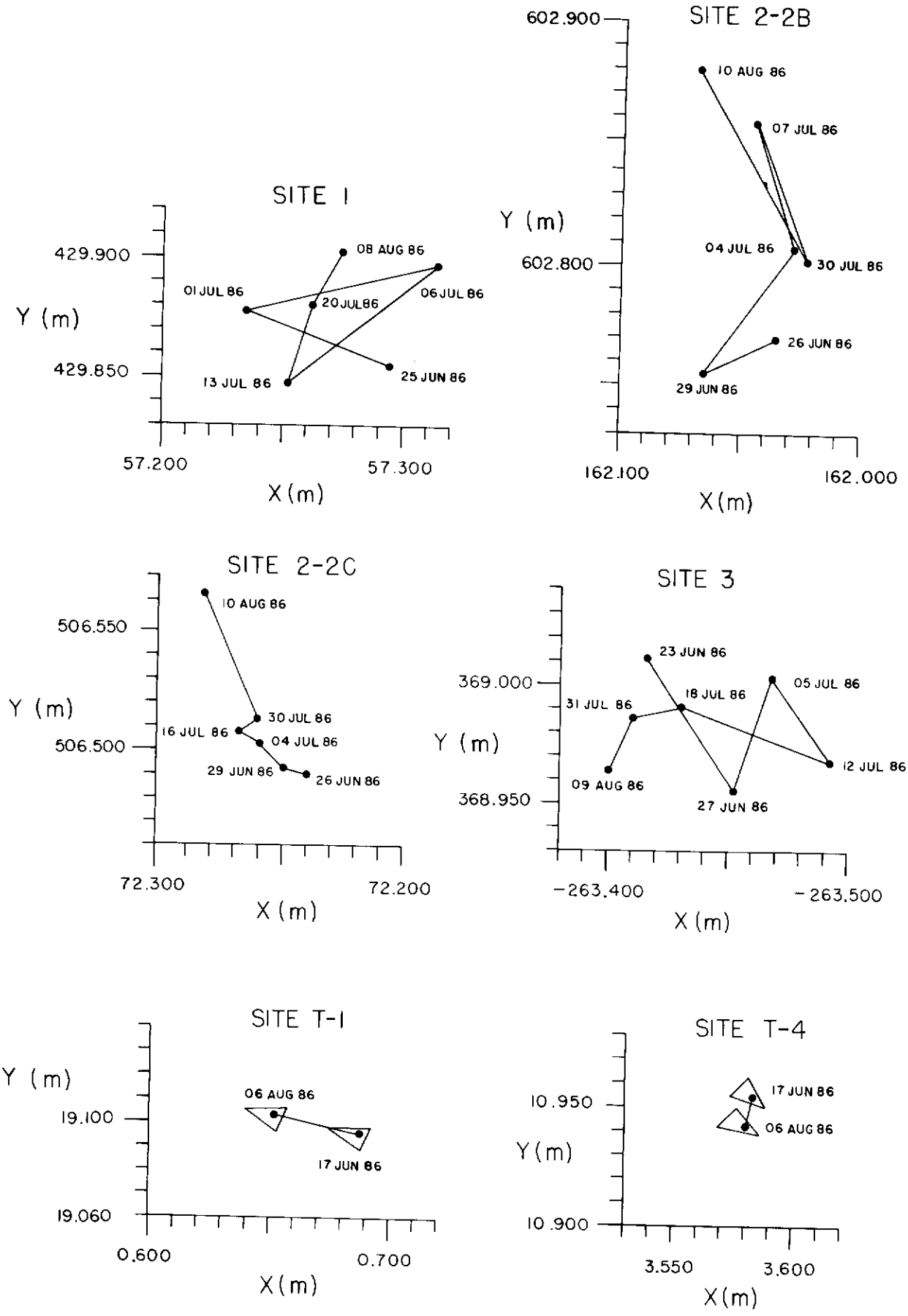

Figure 8. Absolute and relative displacement of survey points on the main slide mass. Date of measurement and position of the points relative to fixed origins are recorded.

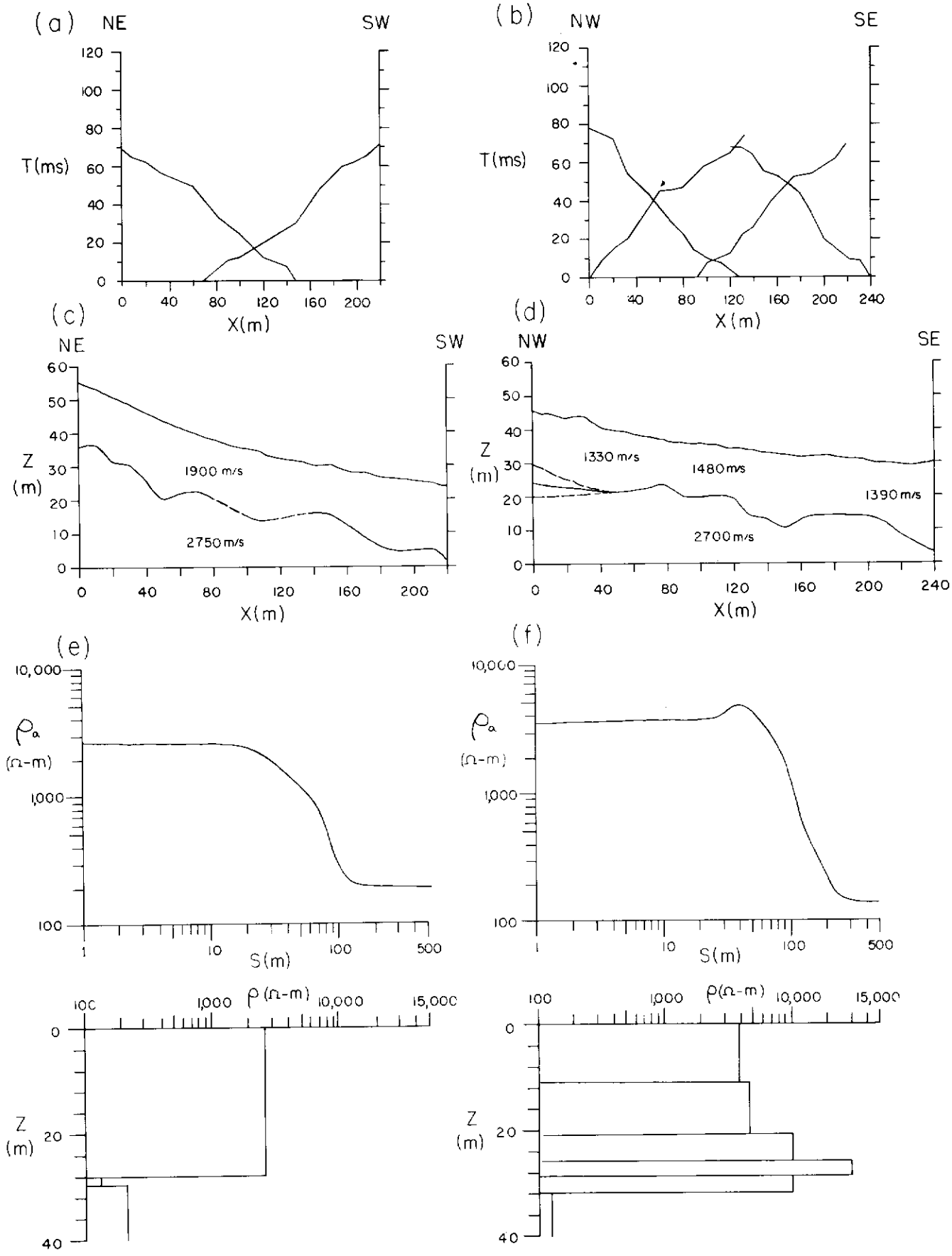

Figure 9. Results of geophysical surveys conducted on main slide. (a) - (b) Travel-time curves for seismic refraction surveys. (c) - (d) Profiles of ground surface and seismic refractors along each line. (e) - (f) Apparent resistivity curves at sites A and B respectively. Best-fit models are shown beneath with the resistivity and depth of each layer indicated.

develops there, and groundwater can be perched at this level. The juxtaposition of fractured low velocity material over intact high velocity material presents a situation where the interface between them can be mapped using the seismic refraction technique. Electrical resistivity soundings can detect perched groundwater as a conductive layer. For an ideal single rupture surface, electrical resistivity and seismic surveys should complement each other, with a conductive layer being detected immediately above a seismic refractor. At Cement Creek, geophysical surveys failed to detect the rupture surface at depth because of instrumental limitations and interference of permafrost.

Seismic refraction surveys were conducted using a Bison 1570B single channel seismograph and a maximum shot-geophone spacing of 150 m. A 4.5 kg sledgehammer and plate set and explosives were used as energy sources. Poor transmission properties of the surficial cover rendered the hammer useless at spacings greater than 60 m and necessitated the use of up to 3 sticks of 60% Forcite at end of line shots. A shot spacing of 10 m was used on each of the three lines shown in Figure 7. A test section was run at survey station 1 to determine the electrical cap delay time and to determine velocities in the Wrangell Lavas. Two section lines were on the landslide, oblique to the inferred dip of the rupture surface. Travel time curves for these lines are shown in Figure 9a-b.

The data was inverted using the method of Wyrobek (1956) which was selected because only a single refractor, subparallel with the surface, was detected. Cross sections along seismic lines shot on the slide, showing both ground surface and refractor topographies are displayed in Figure 9c-d. Depths to the refractor are considered accurate to within 10%. Significant changes in the velocity of the upper layer were apparent in the NW-SE section while that of the NE-SW line was constant. The velocity of the lower layer remained essentially constant along both lines.

The average depth to the refractor, between 15 and 20 m, was too deep to explain it as being the base of frozen surficial deposits since shots frequently exposed bedrock at 0.5 m depths. The refractor seems to represent the base of a combined layer of weathered rock and surficial cover. The anisotropic velocity profile of the upper layer along the NW-SE line most likely relects the presence of ground cracks; this line is transverse to them, while the NE-SW line parallels ground failure and does not intersect any major cracks. The absence of velocity anisotropy in the layer below suggests that ground failure is confined to a layer of weathered rock and till. The seismic profiles did not cross any of the deep cracks which subdivide the slide into major blocks. The ground failure along the seismic profiles may therefore have resulted from strong ground motion during the 1983 landslide. This mechanism may also explain the ground failure immediately west of the landslide.

Electrical reistivity soundings were conducted at two sites using an expanding Schlumberger array and apparatus built at the University of Alberta. Current electrode spacing was expanded in increments of 20 m with potential electrode spacing being widened when the measured voltage dropped below 4.0 mV. Apparent resitivity profiles for the two sites are shown in Figure 9e-f.

The results were inverted using a resistivity transform technique suggested by Koefoed (1979) since more than two layers were apparent in the profile at site B and master curves for such cases are not readily available. The method involved comparison of actual and model values of the resistivity transform function at selected values of the current electrode spacing (s). The data was sampled at s-intervals of six per decade and converted into values of the resistivity transform by the application of a digital filter developed by O'Neill (1975). Model parameters were then specified and values of the resistivity transform for corresponding spacings were calculated using the Pekeris Recurrence Relations (Pekeris, 1940). The model was adjusted until the transform values of the data and the model agreed within 2%. Best fit models for sites A and B are displayed immediately below their corresponding apparent resistivity profiles.

The resistivity profiles seem to delineate the lower limit of permafrost in the slide mass. The abrupt change in resistivity at around 30 m does not correspond with either the base of the weathered rock layer or with any reasonable projection of the rupture surface at depth. The most likely interpretation of the models is that they delineate an upper layer of frozen, high resistivity rock and till underlain by thawed rock whose resistivity has been lowered by jointing and clay alteration. The difference in upper layer resistivity between sites A and B is probably due to greater hydrothermal alteration of rock at site A; hydrothermal alteration of rock exposed in the headwall scarp decreases from east to west. The effect of clay alteration on rock conductivities has been summarized by McNeill (1980). Bound water in clay minerals allows relatively high rock conductivities to persist below the freezing point because electrolytes inhibit bound water from freezing and allow current paths to remain open.

The resistivity soundings indicate that groundwater near the rupture surface is unlikely to freeze at any time. Groundwater seepage was observed from portions of the landslide toe during the summer of 1986. Saturated conditions could develop near the base of the landslide once freeze-up has occurred and might persist for a considerable period. By lowering the effective shear strength of the rock, trapped groundwater may play an important role in preparation of the landslide for failure.

CONCLUSIONS

Landsliding at Cement Creek is confined to lower Wrangell Lavas in the core of a synclinal pericline. Hydrothermal alteration of flow-top breccias has lowered the mechanical stength of these beds and shear failure is largely localized along them. Jointing controlled the location of major ground cracks and a portion of the headwall scarp. Non-cylindrical folding of bedding imparted a rotational component of motion to the slide mass and this is reflected in current displacement vectors and in the pattern of cracks in the slide mass. The 1983 landslide was a single low-velocity block slide with maximum displacement of approximately 40 m. Debris in the toe appears to have arrested the slide although blocks near the head are creeping towards the toe at about 5 $\pm$ 3 cm per month, perhaps on a seasonal basis. The area involved in the 1983 slide has undergone minor mass movement prior to 1943 and probably has been stable for the past century.

Trapped groundwater may have prepared the slide mass for failure with such instability developing after freeze-up when permeablility in the toe of the slide was minimal. Local seismicity may have provided a trigger; the landslide is 300 m south of a major fault in a seismically active area. A single low magnitude event or a series of them could have initiated creep which accelerated into catastrophic failure. If shallow ground failure on and immediately adjacent to the landslide is ascribed to strong ground motion, the slide must have occurred in a matter of seconds.

ACKNOWLEDGEMENTS

This work was supported by D.I.A.N.D. contract Y6-MG02 and by funds from a Natural Sciences and Engineering Research Grant to D.I. Gough. The author wishes to thank D.I. Gough and P. Erdmer for help received in the planning and conduct of field work. P. Von Gaza rendered capable assistance in the field. X-Ray diffraction work was performed by G. Speirs. The author benefited from discussions with A. Peterson, T Skulski and D. Cruden. E. Nyland provided help throughout this work and reviewed this paper.

REFERENCES

CAMPBELL, R.B. and DODDS, C.J., 1979. Operation St. Elias, British Columbia; in Current Research Part A. Geological Survey of Canada, Paper 79-1A, p. 17-20.

CAMPBELL, R.B. and DODDS, C.J., 1978. Operation St. Elias, Yukon Territory; in Current Research Part A, Geological Survey of Canada, Paper 78-1A, p. 35-41.

CLAGUE, J.J., 1979. The Denali Fault System in southwest Yukon Territory - A geologic hazard?; in Current Research Part A, Geological Survey of Canada, Paper 79-1A, p. 50-56.

DODDS, C.J., 1979. Geology of the southwest Kluane Lake map area; Geological Survey of Canada, Open File 829 (Map).

DRYSDALE, J.A., HORNER, R.B. and WETMILLER, R.J., 1983. Canadian Earthquakes - National Summary January - March, 1983; Seismological Services of Canada, Earth Physics Branch.

EISBACHER, G.J., 1975. Operation St. Elias, Yukon Territory: Dezadeash Group and Amphitheatre Formation; in Current Research Part A, Geological Survey of Canada, Paper 75-1A, p. 60-61.

HORNER, R.B., 1983. Seimicity in the St. Elias Region of Northwestern Canada Bulletin of the Seismological Society of America, Vol. 73, No. 4, pp. 1117-1137.

KOEFOED, O., 1980. Geosounding Principles, 1 (Resistivity Sounding Measurements); New York, Elsevier.

LAHR, J. and PLAFKER, G., 1980. Holocene Pacific - North American Plate interaction in Southern Alaska: implications for the Yakataga Seismic, Gap; Geology, Vol. 8, p. 483-486.

MCNEILL, J.D., 1980. Electrical Conductivity of Soils and Rocks; Technical Note TN-5, Geonics Ltd.

MULLER, J.E., 1967. Kluane Lake Map Area, Yukon Territory; Geological Survey of Canada, Memoir 340.

MULLER, K., 1977. Geophysical methods in the investigation of slope failures; International Association of Engineering Geology Bulletin, Vol. 16, p. 227-229.

NATIONAL EARTHQUAKE FORMATION SERVICE (NEIS), 1983. Preliminary determination of epicenters - March, 1983.

O'NEILL, D.J., 1975. Improved linear filter coefficients for application in apparent resistivity computations; Bulletin of Australian Society of Exploration Geophysicists, Vol. 6., p. 104-109.

PERKERIS, C.L., 1940. Direct method of interpretation in resistivity prospecting; Geophysics, Vol. 5, p. 31-46.

READ, P.B. and MONGER, J.W.H., 1975. Operation St. Elias, Yukon Territory: The Mush Lake Group and Permo-Triassic rocks in the Kluane Ranges; in Current Research Part A, Geological Survey of Canada Paper 75-1A, p. 55-59.

SKULSKI, T. and FRANCIS, D., 1986. On the Geology of the Tertiary Wrangell lavas in the St. Clare Province, St. Elias Mountains, Yukon; in Yukon Geology Vol. 1; Exploration and Geological Services Division, Yukon, Indian and Northern Affairs Canada, p. 161-170.

SOUTHER, J.G. and STANCIU, C., 1975. Operation St. Elias, Yukon Territory: Tertiary Volcanic Rocks; in Current Research Part A, Geological Survey of Canada Paper 75-1A, p. 63-70.

STEPHENS, C.D., FOGLEMAN, K.A., PAGE, R.A. and LAHR, J., 1985. Seismicity in southern Alaska, October, 1982 - September, 1983; in Bartsch-Winkler S. and Reed, K.M. (eds), The United States Geological Survey in Alaska - Accomplishments during 1983, United States Geological Survey, Circular 945, p. 83-86.

TER STEPANIAN, G., 1980. Measuring displacements of wooded landslides with trilateral signs; Proceedings of the International Symposium on Landslides, Vol. 1, New Delhi: Sarita Prakashan.

WYROBEK, S.M., 1956. Application of delay and intercept times in the interpretation of multilayer refraction time distance curves; Geophysical Prospecting, Vol. 4, p. 112-130.